ISSN: 2155-9864
Journal of Blood Disorders & Transfusion

OPEN ACCESS Freely available online

Research Article

Computer-Assisted Aneurysm Growth Evaluation and Detection (AGED): Comparison with Clinical Aneurysm Follow-Up

Aichi Chien[1*], Ziga Spiclin[2], Ziga Bizjak[2], Kambiz Nael[1]

[1]Department of Radiological Science, David Geffen School of Medicine at UCLA, 10833 Leconte Ave, Box 957350 Los Angeles, CA 90095, USA; [2]University of Ljubljana, Department of Electrical Engineering, SI-1000 Ljubljana, Slovenia

ABSTRACT

Background: Since growing Intracranial Aneurysms (IA) are more likely to rupture, detecting growth is an important part of unruptured IA follow-up. Recent studies have consistently shown that detecting IA growth can be challenging, especially in smaller aneurysms. In this study, we present an automated computational method to assist in aneurysm growth detection.

Methods: An analysis program, Aneurysm Growth Evaluation and Detection (AGED), based on IA images was developed. To verify the program can satisfactorily detect clinical aneurysm growth, we performed this comparative study using clinical determinations of growth during IA follow-up as a gold standard. Patients with unruptured, saccular IA followed by diagnostic brain CTA to monitor IA progression were reviewed. 48 IA image series from 20 longitudinally-followed ICA IA were analyzed using AGED and a set of IA morphologic features were calculated. Nonparametric statistical tests and ROC analysis were performed to evaluate the performance of each feature for growth detection.

Results: The set of automatically calculated morphologic features demonstrated comparable results to standard, manual clinical IA growth evaluation. Specifically, automatically calculated HMAX was superior (AUC=0.958) at distinguishing growing versus stable IA, followed by V, and SA (AUC=0.927 and 0.917, respectively).

Conclusion: Our findings support automatic methods of detecting IA growth from sequential imaging studies as a useful adjunct to standard clinical assessment. AGED-generated growth detection shows promise for characterization and detection of IA growth with potential to decrease variability associated with manual measurements.

Keywords: Unruptured intracranial aneurysms; Computer-assisted growth detection; Surface mesh reconstruction; Computed tomography angiography; Morphologic neuroimaging analysis

Abbreviations: AGED: Aneurysm Growth Evaluation and Detection program; AUC: Area Under the receiver operating characteristic Curve; HMAX: Maximum Aneurysm dome size; dMPL: Differential Median Deformation Path Length; dSA: Differential Surface Area; dV: Differential Volume; dICDD: Differential Integral of Cumulative Deformation Distances, IA: Intracranial Aneurysm; IQR: Inter Quartile Range; ROC: Receiver Operating Characteristic; SAH: Subar Achnoid Hemorrhage

INTRODUCTION

The prevalence of unruptured Intracranial Aneurysms (IA) in the general population is estimated at 2%-8% [1,2]. Although incidence of IA rupture and subsequent SAH is relatively low (about 10-30 per 100,000 per year), the consequences are very often devastating and result in lifelong disability if not death [1]. IA treatment to prevent rupture has become increasingly safer with the widespread use of interventional approaches and intravascular devices [3,4]. Despite improvements, treatment options remains expensive and is not without its own complication risks. Further, since only a

Correspondence to: Aichi Chien, Department of Radiological Science, David Geffen School of Medicine at UCLA, 10833 Leconte Ave, Box 957350 Los Angeles, CA 90095, E-mail: aichi@ucla.edu

Received: 28-Jul-2022, Manuscript No. JBDT-22-17578; **Editor assigned:** 01-Aug-2022, Pre QC No. JBDT-22-17578 (PQ); **Reviewed:** 16-Aug-2022, QC No. JBDT-22-17578; **Revised:** 24-Aug-2022, Manuscript No. JBDT-22-17578 (R); **Published:** 02-Sep-2022, DOI: 10.4172/2155-9864.22.13.517

Citation: Chien A, Spiclin Z, Bizjak Z, Nael K. (2022) Computer-Assisted Aneurysm Growth Evaluation and Detection (AGED): Comparison with Clinical Aneurysm Follow-Up. J Blood Disord Transfus. 13:517.

small percentage of unruptured IA go on to rupture, the ability to accurately identify those with a higher risk of rupturing is essential for informed clinical decision-making as well as to avoid recommending unnecessary procedures.

Current clinical practice leans towards preventative treatment for IA with diameters greater than 7 mm and smaller IA which demonstrate growth, with exceptions made for those with biological risk factors such as advanced patient age [4]. Therefore, for small unruptured IA, monitoring for interval growth through imaging follow-up is essential for IA management. However, performing IA size measurements to detect growth can be a time-consuming task as it is performed manually. In addition, small IA typically have proportionally small changes in size, and it may be necessary to check the IA from multiple angles. One important limitation of our current methods of aneurysm measurement is intra- and inter observer variability. Depending on the imaging modality and observer, one study reported a wide range of correlation coefficients (ranging from 0.85 to 0.98) for interobserver measurements, which represents as much as a 17% difference in IA size [5]. Although not directly comparable to Kim's values due to methodological differences, Villablanca et al. found intra observer differences (0.984-0.987) to be even larger than interobserver differences (0.994-0.997) [6]. This difference in agreement between and within observers demonstrates a clear lack of consistency.

Detecting IA growth is an essential part of IA management and a determinant in risk assessment and subsequent treatment decision. Past studies have linked IA growth to rupture [6]. A meta-analysis of 15 studies that investigated unruptured IAs and involved longitudinal monitoring using follow-up imaging found that the definition of size change measurements and associated growth thresholds varied substantially among studies [7]. For instance, size changes were characterized as changes in maximum dome diameter, maximum transverse dome diameter, increase in any dimension or increase in greatest diameter [8-13]. The assessment of growth was performed using manual measurement tools on 2D or 3D images and some included qualitative evaluation of IA shape and the appearance of blebs or lobes. To account for variations between manual measurements, different studies also have different growth thresholds, ranging from 0.5 mm to 2 mm. In spite of the variations in the growth detection thresholds, these studies concluded that IA growth is highly correlated to rupture, shedding light on the importance of aneurysm growth as a key prognostic factor. This knowledge has increased the number of unruptured IA followed through imaging. However, in the clinical setting, the standard technique of detecting IA growth in follow-up images still relies on time-consuming and somewhat subjective manual methods of taking and comparing multiple measurements.

In this research, we propose an automatic computational tool for aneurysm growth detection to provide quick, repeatable and consistent measurements. We present Aneurysm Growth Evaluation and Detection (AGED) to analyze aneurysm follow-up images. Our approach builds on previously described methods to automatically define the IA neck and quantify IA morphologic characteristics [14]. We also utilize a shape morphing approach to automatically map the initial images and follow-up images and quantify differences. The automatic computed output of AGED to determine growth is compared against the clinical reads/measurement obtained by board certified neuroradiologists.

MATERIALS AND METHODS

Case information

This retrospective study was approved by the UCLA Institutional Review Board (UCLA IRB). This research was performed in accordance with relevant guidelines and regulations. As approved by the UCLA IRB for this retrospective study, informed consent was waived for all participants included in this research. Medical records for patients who had longitudinal imaging studies to monitor unruptured IA from 2005-2010 were reviewed. There were total of 235 patients who had unruptured IA followed by image studies during this period of time. For these patients, CTA follow-up image series were acquired with matrix size 512 × 512, field of view 180 mm, in-plane pixel size 0.39 mm, and section thickness 1.0 mm [6]. Among the follow-up IA cases, 180 were located at the ICA (18 growth, 162 stable), 56 ACA (6 growth, 50 stable), and 60 MCA (12 growth, 48 stable). To study the accuracy of automatic analysis by AGED and minimize potential bias due to case selection, IA from ICA locations with similar imaging interval were selected to provide balanced case numbers in the growth and stable groups.

Image processing and analysis

From each 3D CTA imaging study, the IA was manually located, marching cubes and smooth non-shrinking algorithms were applied for segmentation and extraction of the IA and parent artery 3D surface mesh [15,16]. Figure 1 shows the aligned initial and follow-up IA shapes separated by clinical growth/stable classification. Following segmentation, the surface mesh comprising the IA was isolated from the parent vessel using an Automated Cutting Plane (ACP) method [14]. The isolated IA shape was used to compute the morphologic features. Morphologic features were computed using two general approaches. In the first approach, morphologic features were extracted directly using initial and follow-up IA meshes. Based on ACP methods, IA Surface Area (SA), Volume (V), and Maximum Aneurysm dome size (HMAX) were calculated. Although similar to the manual clinical measurement of maximum diameter, because it is a computational analysis, HMAX effectively measures all possible directions in 3D to find the maximum distance in a fraction of a second. The relative change for each feature was computed by subtracting the initial and follow-up IA values: (follow-up value-initial value)/initial value. The second approach was based on morphing calculations to estimate the path of IA growth from initial to follow-up. We implemented this morphing calculation to test if it provided better growth detection by considering the intermediate shapes between the initial and follow-up image (Figure 2). We utilized a two-stage morphing approach beginning with rigid alignment followed by non-rigid mesh-to-mesh deformation to compute differential features including Median deformation Path Length (dMPL), differential Surface Area (dSA), differential Volume (dV), and differential Integral of Cumulative Deformation Distances (dICDD) [17]. The calculation of these morphologic features is illustrated and summarized in Figure 2.

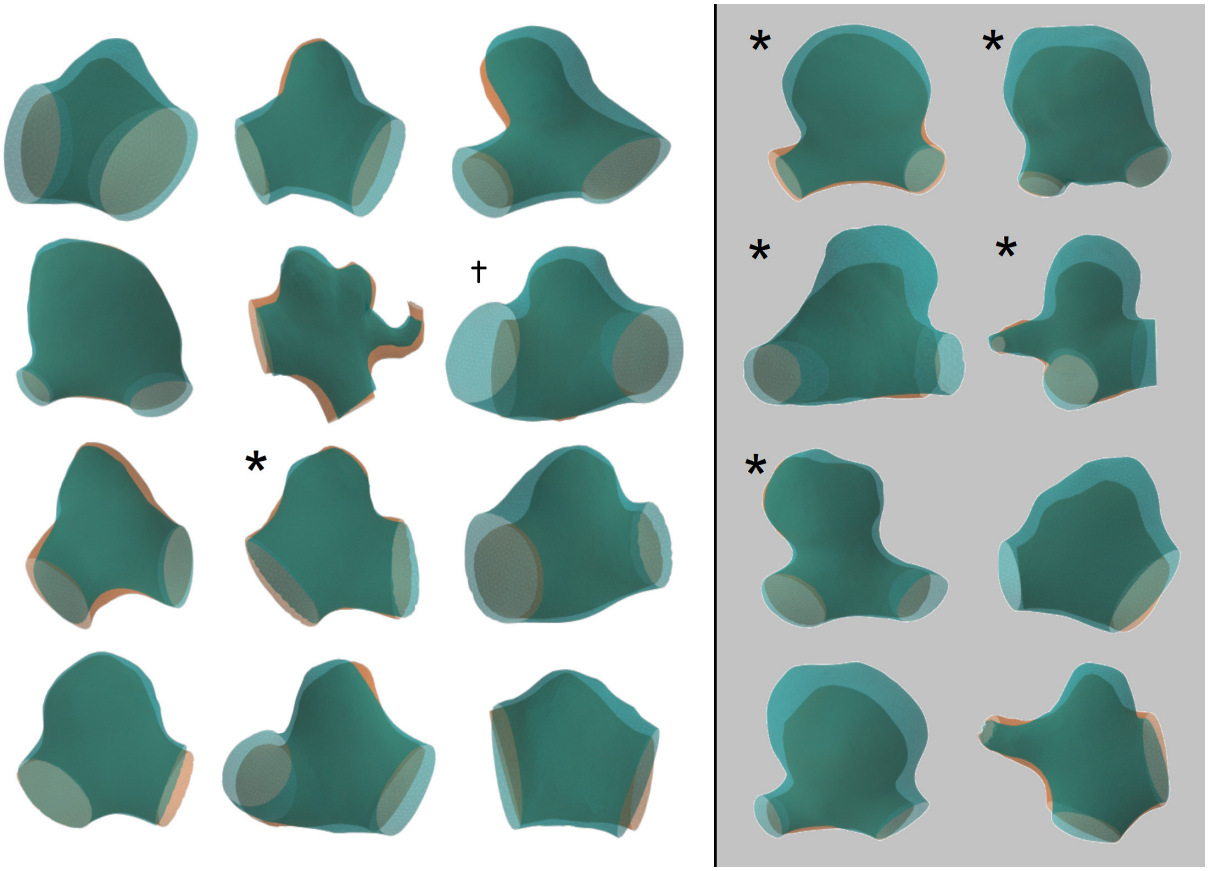

Figure 1: 3D reconstructions of IA based on initial images (orange) and follow-up images (green) shapes. Based on clinical IA follow-up measurements, stable IAs is shown on the left and growing IAs is shown on the right. Asterisks (*) mark aneurysms treated at some point after the follow-up imaging. The dagger (†) labels an aneurysm for which the two time points had different imaging thresholds so that overall the aneurysm and vessel appear larger. However, both clinical evaluation and AGED showed the aneurysm did not grow, as both approaches considered overall morphology changes with respect to the vessel. **Note:** (——) 3D reconstructions of IA based on initial images, (▬) 3D reconstructions of IA based on follow-up images

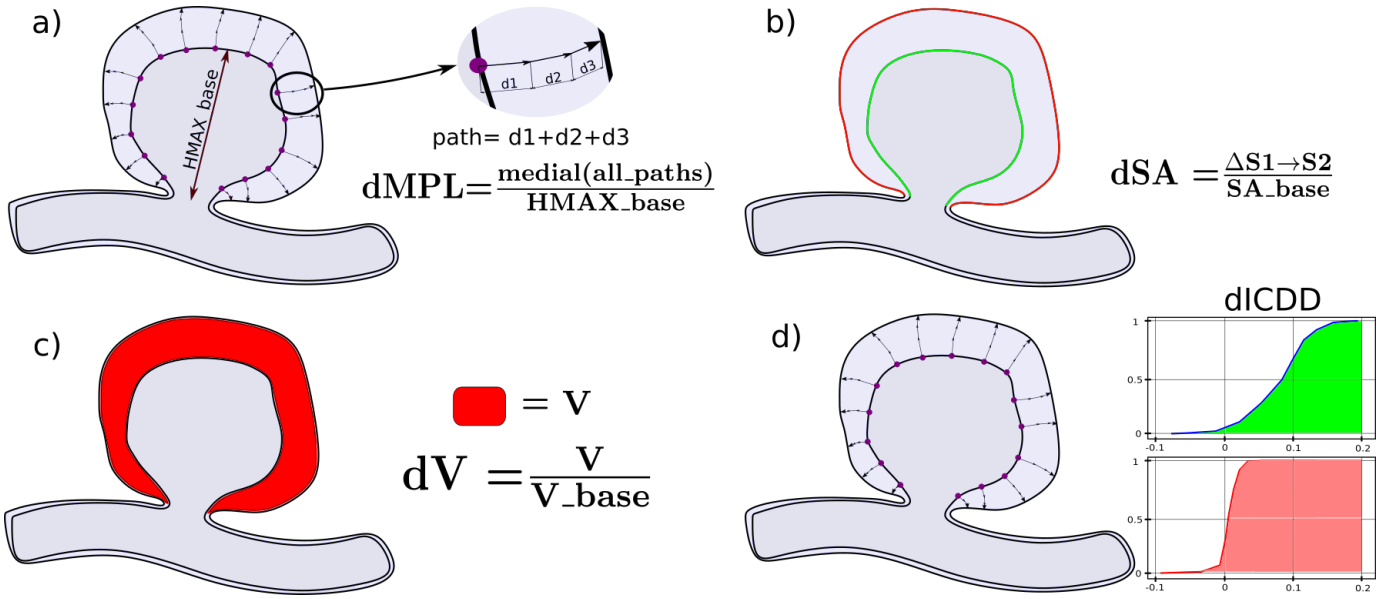

Figure 2: Graphic presentation of four novel features for AGED morphing analysis to quantify IA changes: a) Differential Median deformation Path Length (dMPL), accumulates the deformation paths of all vertices that represent the initial IA shape, normalized by dividing by initial HMAX. b) Differential Surface Area (dSA), surface change between deformed and initial IA dome surface mesh divided by initial IA dome surface mesh. c) Differential Volume (dV), volume changes between deformed and initial IA divided by initial IA volume. d) Differential Integral of Cumulative Deformation Distances (dICDD), area under the curve of cumulative distribution functions of growth paths.

The outcome of AGED was compared against clinical reads obtained by board certified neuroradiologists. The measurements are made in a dedicated 3D Lab by applying multiplanar reformations using dedicated software (Vital Images, Minneapolis, Minn). This data is recorded in our aneurysm data registry and used as the reference of standard [6].

Statistical analysis

For each feature, we computed the median and Inter Quartile Range (IQR). These are reported in the text in the format of median (IQR). To compare the groups, we used the non-parametric 2-sided Mann–Whitney U test, and to quantify the performance classifying the cases we used the Area Under the Curve (AUC) value computed from Receiver Operating Characteristic (ROC) curve. For categorical variables, the 2-sided Chi-Square Test was used. Correlations were assessed using Kendall's tau-b. The statistical significance threshold was set as p-value <0.01.

RESULTS

The IA cases used in this study for comparative analysis, at initial imaging, recorded IA sizes were a median of 3.85 mm. The time interval between the initial scan and follow-up scans was a median of 2.5 years. To verify the study sample is unbiased, statistical analysis between groups was performed. Specifically, IA cases' anatomical locations, baseline sizes, and imaging intervals were not significantly different between groups. Patient characteristics, such as age at IA detection, family history of SAH, history of stroke or TIA, hypertension, thyroid disease, cancer, and atherosclerosis were also not significantly different between the groups. These results verify that the IA characteristics and patient characteristics were not different between groups when IA follow-up images were analyzed by clinical gold standard measurements. Therefore, using clinical gold standard follow-up IA measurements for these cases as a baseline comparison is appropriate to verify AGED accuracy in detecting IA growth in follow-up images (Table 1).

The IA growth analysis from clinical standard IA image measurements and results of different size related features computed by AGED. The analysis showed that AGED automatically computed features are comparable to gold-standard manual measurement for determining growth. The computer analysis shows promising results to detect growth specifically with automatically computed features using direct comparison between initial and follow-up IA images. Specifically, AGED using ACP analysis, the changes of HMAX, V, and SA showed promising results to detect growth (p=0.0002, 0.001, and 0.001, respectively) (Table 2). According to ROC analysis, high classification scores of AUC=0.958, 0.927, and 0.917 were achieved by HMAX, V, and SA, respectively (Table 2 and Figure 3). With the AGED morphing analysis, dSA, which estimates the expansion of the aneurysmal wall surface area, was closest to statistically significant in detecting growth (p=0.056). According to ROC analysis, dSA had a relatively low AUC=0.865 compared with features HMAX, V, and SA. Other morphing features such as dMPL, dV, and dICDD were less effective at statistically differentiating growth and stable IA.

Tukey box-whisker plots of the clinical measurement for growth and stable groups and AGED automatically calculated morphologic values for different features. In general, higher values indicated growth for all factors except dICDD, including clinical size, HMAX, V, SA, dMPL, dV, and dSA. Overlap between the tails indicates a small degree of uncertainty when detecting growth, even with clinical size measurements (Figure 4). Taking the scale bar for each feature in Figure 4 into account, features computed with the morphing approach show greater overlap between stable and growth IA, suggesting they are not as efficient at detecting growth (differentiating growth and stable IAs).

Table 1: Summary of cases to verify AGED against gold standard clinical IA growth evaluation.

	Total	Stable	Growth	p-value
Number of Patients	20	12	8	
Patient Age (years)	69.8 (16.2)	68.5 (17.2)	69.8 (14.7)	0.734
Imaging Interval (years)	2.50 (2.75)	2.50 (4.75)	2.50 (1.0)	0.792
Initial image aneurysm Size (mm)	3.85 (4.30)	3.45 (3.95)	6.15 (6.25)	0.384
FU Max Size (mm)	6.10 (7.38)	3.85 (3.63)	8.40 (8.08)	0.025
IA Treated	6	1	5	0.018
Aneurysm Location				0.161
ICA- Anterior Circulation	14	10	4	
ICA-Posterior Communicating Artery	6	2	4	
Family History of SAH	1	1	0	0.600
Stroke or TIA	3	1	2	0.344
Hypertension	9	5	4	0.535
History of Smoking	3	3	0	0.193
Thyroid Disease	2	2	0	0.347
Cancer	4	2	2	0.535
Atherosclerosis	13	9	4	0.251

Note: Results are presented as median and Inter Quartile Range (IQR), Median

Table 2: Statistical differences between growing and stable IA. Each feature represents normalized change between two imaging points.

	Stable IA	Growth IA	Mann-Whitney U statistic	Mann-Whitney U Significance (p)	ROC Area Under the Curve
Clinical measurements	-0.005 (0.094)	0.254 (0.340)	85	0.004	0.927
HMAX	-0.016 (0.167)	0.224 (0.264)	92	0.0008	0.958
V	0.087 (0.360)	1.07 (1.09)	89	0.004	0.927
SA	0.056 (0.240)	0.501 (0.480)	88	0.006	0.917
dMPL	0.027 (0.041)	0.066 (0.068)	74	0.175	0.771
dSA	0.100 (0.206)	0.691 (0.522)	83	0.056	0.865
dV	0.211 (0.407)	1.08 (1.03)	78	0.080	0.812
dICDD	0.648 (0.120)	0.494 (0.165)	17	0.080	0.823

Note: Results are presented as median and Inter Quartile Range (IQR), Median

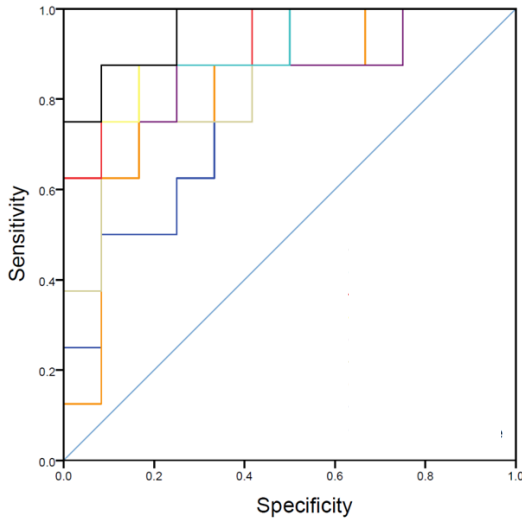

Figure 3: ROC Curve for features for classification of IA growth relative to clinical determination. AUC are values provided in Table 2. **Note:** (——) HMAX, (——) V, (——) Clinical Size SA, (——) dSA, (——) dICDD, (——) dV, (——) dMPL, (——) Reference Line.

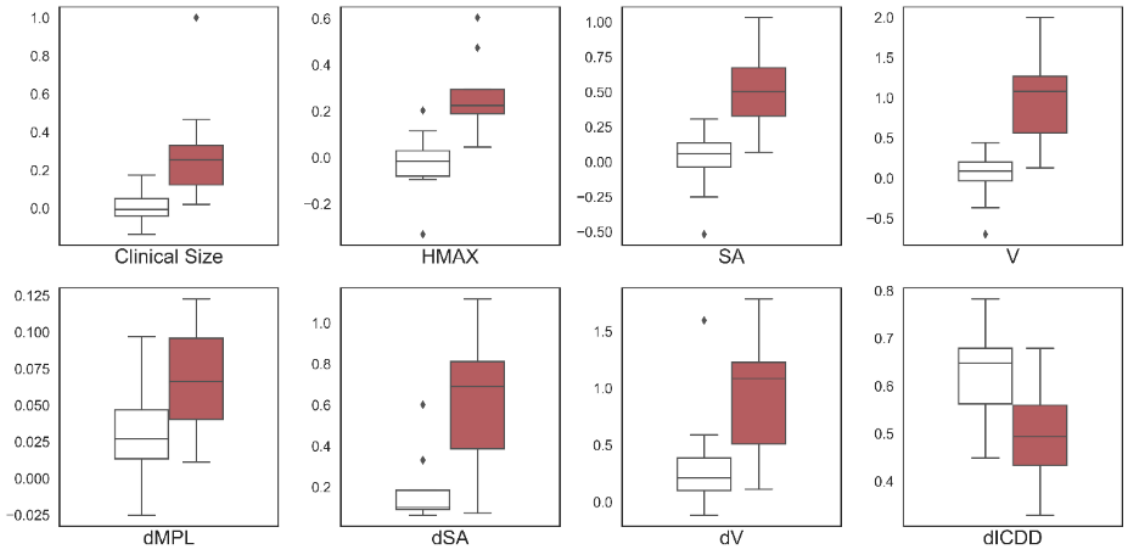

Figure 4: Tukey box-whisker plots for the stable (white) and growing (red) IA groups and morphologic features. Outliers are indicated with diamonds. Features are presented as changes normalized with respect to value obtained from initial IA. HMAX, V, and SA obtained from ACP approach and dMPL, dSA, dV and dICDD obtained by morphing approach.

DISCUSSION

Studies have shown the importance of monitoring aneurysm growth because growing aneurysms have higher risk of rupture. Many studies looking at IA growth primarily focus on the prediction of growth [4,9,18]. For example, Chien, et al. reported the ability of IA volume, surface area, size ratio and NSI to predict growth [18]. A recent retrospective study investigated various clinical scores (PHASES, UCAS, and ELAPSS) to predict IA growth [19]. Although these studies provide risk stratification that can help identify high risk IAs and subsequently guide treatment and surveillance planning, there are limited resources to detect IA growth using follow-up imaging. Our approach presents an automatic computation to detect IA growth in follow-up imaging that enables consistent, reliable and timely analyses.

Currently, follow-up IA images need to be carefully compared with initial images, and manual measurements and morphologic evaluation are commonly performed to detect growth. Resulting measurements commonly vary both between observers and when an individual observer makes repeat measurements [5,6]. The AGED program is designed to automatically assess measurement standards and use 3D analysis techniques to detect growth based on computational methods. In the present study we found that many of the automatically computed features-HMAX, V, SA-had comparable performance to the standard clinical measurements to detect growth. Specifically, HMAX provided superior accuracy in growth evaluation. This is likely because the feature HMAX computes maximum distance in 3D IA images similarly to the clinical standard. It should be noted that HMAX is an automated, objective assessment and is generated within a fraction of a second. Implementing HMAX may be a useful addition to clinical IA evaluation while clinicians perform critical review of aneurysm blebs or irregular shapes.

In this study, we employed the longitudinal IA shape, ACP and morphing analysis methods to calculate various IA growth-related features. Shape morphing deforms the IA surface mesh extracted from the initial scan into the shape extracted from the follow-up scan. The result of shape morphing is an interdeformation field that maps how the baseline shape develops into the follow-up one. We found stronger correlation between the method of feature computation (SA and V (0.947, $p<0.01$), dSA and dV (0.821, $p<0.01$)) than the corresponding features (SA and dSA (0.474, $p<0.01$), V and dV (0.389, $p=0.016$), indicating that the computational method affected how well the features were able to detect growth. This further suggests that the change in surface area calculated with the morphing approach (dSA) may differ from that calculated by comparing surface area directly (SA). Since the morphing analysis assumes the surface mesh changes under a mathematical function, further study to investigate the relationship between SA and dSA with longer follow-up time may be useful to understand whether there are local IA wall changes (such as bleb formation) which challenge the morphing approach. In such a case, the resulting morphing-estimated IA surface wall change may be smaller than the actual wall change. Localized or regional changes in IA wall during growth are known to occur related to hemodynamics or local wall damage [20]. Differences between the calculation methods may indicate specific local wall damage which has weakened the wall and caused certain regions to grow at different rates.

The AGED morphing approach to identify changes in follow-up imaging is relatively new to IA, but similar techniques have been previously applied to other biological problems [21,22]. In this study we compared two novel features that characterize the deformation field, the first being median deformation path length normalized by baseline aneurysm size (dMPL), and second the integral of cumulative deformation distances (dICDD). These two features did not show satisfactory performance to detect growth, likely due to these features simplifying the complex deformation field to a single value. dMPL and dICDD is to analyze small changes in the growth path, further improvement of these feature analyses for specific regions of IA growth may provide new information related to regional growth characteristics and the details of IA growth [17].

Limitations

The main challenges for detecting IA growth are the small sizes of IAs most commonly found and the limited resolution capabilities of current imaging modalities. Therefore, the technique to detect growth needs to be robust enough in order to reliably ascertain small but clinically relevant changes between initial IA images and follow-up images. We studied a group of IA with clinical follow-up studies to verify that the ability of AGED to detect IA growth is comparable to clinical measurements. Additional studies with longer follow-up and greater sample size of IA in various anatomical locations can further verify the program's accuracy and evaluate performance of different features.

CONCLUSION

There is an unmet need for objective quantification tools in the IA management pipeline. Particularly in the cases of small IAs where minor changes can be difficult to discern but may mean the difference between life-saving and life-threatening. In this study, we applied a computational approach for detection of morphologic changes in unruptured IA to assess growth. Morphologic features computed from longitudinal image studies provided fast, automated results that are comparable to current manual assessment of IA growth while eliminating the inherent variability and biases of manual analysis.

ACKNOWLEDGEMENT

All authors made substantial contributions to the conception or design of the work, acquisition, analysis, and interpretation of data, drafted and revised the work, approved the version to be published; and agree to be accountable for all aspects of the work in ensuring that questions related to the accuracy or integrity of any part of the work are appropriately investigated and resolved.

FUNDING STATEMENT

This research was supported in part by National Institutes of Health, National Heart, Lung, and Blood Institute under award number R01HL152270 and American Heart Association Innovative Project Award 18IPA34170130.

CONFLICTS OF INTEREST

The authors declare that there are no conflicts of interest regarding the publication of this paper.

Ethics approval

This work is approved under UCLA IRB review board review.

Consent to participate

The informed consent is waived as it is a retrospective study.

Consent for publication

All authors have read and approved the final manuscript for publication.

REFERENCES

1. Brinjikji W, Zhu YQ, Lanzino G, Cloft HJ, Murad MH, Wang Z, et al. Risk factors for growth of intracranial aneurysms: A systematic review and meta-analysis. AJNR Am J Neuroradiol. 2016;37(4):615-620.
2. Vlak MH, Algra A, Brandenburg R, Rinkel GJ. Prevalence of unruptured intracranial aneurysms, with emphasis on sex, age, comorbidity, country, and time period: A systematic review and meta-analysis. Lancet Neurol. 2011;10(7):626-636.
3. Kotowski M, Naggara O, Darsaut TE, Nolet S, Gevry G, Kouznetsov E, et al. Safety and occlusion rates of surgical treatment of unruptured intracranial aneurysms: a systematic review and meta-analysis of the literature from 1990 to 2011. J Neurol Neurosurg Psychiatry. 2013;84(1):42-428.
4. Thompson BG, Brown RD, Amin-Hanjani S, Broderick JP, Cockroft KM, Connolly ES, et al. Guidelines for the management of patients with unruptured intracranial aneurysms. Stroke. 2015;46(8):2368-400.
5. Kim HJ, Yoon DY, Kim ES, Lee HJ, Jeon HJ, Lee JY, et al. Intraobserver and interobserver variability in CT angiography and MR angiography measurements of the size of cerebral aneurysms. Neuroradiology. 2017;59(5):491-497.
6. Villablanca JP, Duckwiler GR, Jahan R, Tateshima S, Martin NA, Frazee J, et al. Natural History of Asymptomatic Unruptured Cerebral Aneurysms Evaluated at CT Angiography: Growth and Rupture Incidence and Correlation with Epidemiologic Risk Factors. Radiology. 2013;269(1):258-265.
7. Backes D, Rinkel GJE, Laban KG, Algra A, Vergouwen MDI. Patient- and aneurysm-specific risk factors for intracranial aneurysm growth. Stroke. 2016;47(4):951-957.
8. Burns JD, Huston J, Layton KF, Piepgras DG, Brown RD. Intracranial aneurysm enlargement on serial magnetic resonance angiography. Stroke. 2009;40(2):406-411.
9. Ferns SP, Sprengers MES, van Rooij WJJ, van Den Berg R, Velthuis BK, dee Kort GAP, et al. de novo aneurysm formation and growth of untreated aneurysms. Stroke. 2011;42(2):313-318.
10. Juvela S, Poussa K, Porras M. Factors affecting formation and growth of intracranial aneurysms. Stroke. 2001;32(2):485-491.
11. Matsubara S, Hadeishi H, Suzuki A, Yasui N, Nishimura H. Incidence and risk factors for the growth of unruptured cerebral aneurysms: Observation using serial computerized tomography angiography. J Neurosurg. 2004;101(6):908-914.
12. Matsumoto K, Oshino S, Sasaki M, Tsuruzono K, Taketsuna S, Yoshimine T. Incidence of growth and rupture of unruptured intracranial aneurysms followed by serial MRA. Acta Neurochir (Wien). 2013;155(2):211-216.
13. Phan TG, Huston J, Brown RD, Wiebers DO, Piepgras DG. Intracranial saccular aneurysm enlargement determined using serial magnetic resonance angiography. J Neurosurg. 2002;97(5):1023-1028.
14. Jerman T, Pernus F, Likar B, Spiclin Z, Chien A. Automatic cutting plane identification for computer-aided analysis of intracranial aneurysms. IEEE. 2016; 2:1484-1489.
15. Cebral JR, Löhner R. From medical images to anatomically accurate finite element grids. Int J Num Met Eng. 2001;51(8):985-1008.
16. Lorensen WE, Cline HE. Marching cubes: A high resolution 3D surface construction algorithm. ACM Siggraph Comr Gra. 1987;21(4):163-169.
17. Bizjak Z, Jerman T, Likar B, Pernus F, Chien A. Registration based detection and quantification of intracranial aneurysm growth. Proc SPIE; 2019; 10950:33-43.
18. Chien A, Xu M, Yokota H, Scalzo F, Morimoto E, Salamon N. Nonsphericity index and size ratio identify morphologic differences between growing and stable aneurysms in a longitudinal study of 93 cases. AJNR Am J Neuroradiol. 2018;39(3):500-506.
19. Sturiale CL, Stumpo V, Ricciardi L, Trevisi G, Valente I, D'Arrigo S, et al. Retrospective application of risk scores to ruptured intracranial aneurysms: would they have predicted the risk of bleeding? Neurosurg Rev. 2021;44(3):1655-1663.
20. Nordahl ER, Uthamaraj S, Dennis KD, Sejkorová A, Hejčl A, Hron J, et al. Morphological and hemodynamic changes during cerebral aneurysm growth. Brain Sci. 2021;11(4):520.
21. Bône A, Colliot O, Durrleman S. Learning the spatiotemporal variability in longitudinal shape data sets. International Journal of Computer Vision. 2020;128(12):2873-2896.
22. Yushkevich PA, Aly A, Wang J, Xie L, Gorman RC, Younes L, et al. Diffeomorphic Medial Modeling. Inf Process Med Imaging. 2019;11492:208-220.